Limit on the Branching Ratio of $K_L \to \pi^0\nu\overline{\nu}$

M. Weaver, K. Arisaka, D. Roberts, and W. Slater
University of California at Los Angeles, Los Angeles, California 90024

R. A. Briere, E. Cheu, D. A. Harris, A. Roodman, B. Schwingenheuer, Y. W. Wah, B. Winstein, and R. Winston
The Enrico Fermi Institute, The University of Chicago, Chicago, Illinois 60637

A. R. Barker
University of Colorado, Boulder, Colorado 80309

E. C. Swallow
Elmhurst College, Elmhurst, Illinois 60126
and The Enrico Fermi Institute, The University of Chicago, Chicago, Illinois 60637

G. J. Bock, R. Coleman, M. Crisler, J. Enagonio, R. Ford, Y. B. Hsiung, D. A. Jensen, K. S. McFarland, E. Ramberg, and R. Tschirhart
Fermi National Accelerator Laboratory, Batavia, Illinois 60510

E. M. Collins and G. D. Gollin
University of Illinois, Urbana, Illinois 61801

T. Nakaya and T. Yamanaka
Department of Physics, Osaka University, Toyonaka, Osaka 560, Japan

P. Gu, P. Haas, W. P. Hogan, S. K. Kim,* J. N. Matthews, S. S. Myung,* S. Schnetzer, S. V. Somalwar, G. B. Thomson, and Y. Zou
Rutgers University, Piscataway, New Jersey 08855

(E799 Collaboration)

(Received 8 March 1994)

We report on a search for the decay $K_L \to \pi^0\nu\overline{\nu}$ by the Fermilab E799 Collaboration. The partial width for this mode is related in a calculable way to the CP violation parameters of the standard model. In particular, the decay $K_L \to \pi^0\nu\overline{\nu}$ is predicted to proceed almost entirely via a direct CP violating amplitude. No events were observed, allowing us to set an upper limit on the branching ratio of $B(K_L \to \pi^0\nu\overline{\nu}) < 5.8 \times 10^{-5}$ at the 90% confidence level.

PACS numbers: 13.20.Eb, 11.30.Er

The rare decay mode $K_L \to \pi^0\nu\overline{\nu}$ has received considerable attention lately in the search for direct CP violation [1]. In the standard model, the decay rate for this mode is dominated by direct CP violating amplitudes, namely, the electroweak penguin and W box diagrams. These same diagrams are responsible for the CP violating channel expected in the $K_L \to \pi^0 e^+ e^-$ process as well. In the case of $K_L \to \pi^0 e^+ e^-$, the decay amplitude receives contributions from both the CP-odd component (K_2) of the K_L and the CP-even component (ϵK_1), where ϵ is the indirect CP violation parameter in the K^0-$\overline{K^0}$ system. The direct CP violating amplitude (attributed to K_2) is expected to be comparable to [2], or smaller than [3], the indirect CP violating amplitude (attributed to ϵK_1). In the case of $K_L \to \pi^0\nu\overline{\nu}$, however, the indirect CP violating contribution is expected to be roughly 1800 times smaller than the contribution from the direct CP violating amplitude [1]. Hence, observation of $K_L \to \pi^0\nu\overline{\nu}$ events near the predicted decay rate would provide strong evidence for direct CP violation. In the Wolfenstein parametrization of the Cabibbo-Kobayashi-Maskawa matrix [4], the rate for $K_L \to \pi^0\nu\overline{\nu}$ is proportional to η^2 and also depends upon the value of the top quark mass [1]. Values for $B(K_L \to \pi^0\nu\overline{\nu})$ are in the range $(0.4\text{–}11) \times 10^{-11}$ for currently allowable values of η and m_{top} [5], and have a typical value of 1×10^{-11} for $\eta = 0.22$ and $m_{\text{top}} = 120$ GeV/c^2. The only previous search for the decay mode $K_L \to \pi^0\nu\overline{\nu}$ was conducted by the Fermilab E731 Collaboration, which reported an upper limit of 2.4×10^{-4} at the 90% confidence level [6].

The search for $K_L \to \pi^0\nu\overline{\nu}$ presented herein was conducted by the Fermilab E799 Collaboration, whose primary goal was to search for the rare decay $K_L \to \pi^0 e^+ e^-$ [7]. The goal of this analysis was to detect an isolated neutral pion kinematically consistent with a $K_L \to \pi^0\nu\overline{\nu}$ decay. A distinguishing feature of this decay is that the π^0 may have a value for P_t, the momentum of the π^0 transverse to the K_L line of flight, as large as 231 MeV/c; by contrast, neutral pions from common sources such as $K_L \to \pi^0\pi^0\pi^0$ and $\Lambda \to n\pi^0$ decays may have P_t only as large as 139 MeV/c and 104 MeV/c, respectively. Because of the difficulty in detecting $\pi^0 \to \gamma\gamma$ decays and measuring their P_t in an experiment with a large decay region, such as E799, we search for candidate events

0031-9007/94/72(24)/3758(4)$06.00

in which the π^0 underwent Dalitz decay, $\pi^0 \to e^+e^-\gamma$. This allows measurement of the decay position and, consequently, P_t and $m_{ee\gamma}$. Although the use of π^0 Dalitz decays results in reduced sensitivity due to the smaller π^0 branching fraction, these constraints allow us to achieve good separation between signal and background.

Since the experimental signature for $K_L \to \pi^0\nu\bar{\nu}$ consists of identifying one isolated π^0 Dalitz decay, several background processes contribute to the data sample. Among those with π^0's in the final state are the $K_L \to \pi^0\pi^0$, $K_L \to \pi^0\pi^0\pi^0$, $K_L \to \pi^+\pi^-\pi^0$, and $\Lambda \to n\pi^0$ decay modes. The three K_L processes distinguish themselves from the signal mode by the presence of extra photons or charged pions in the final state. The Λ decay mode is kinematically bound to have a value of P_t less than 104 MeV/c, ignoring detector resolution. The semileptonic mode $K_L \to \pi^+e^-\bar{\nu}$ and its charge conjugate, together known as "K_{e3}," contribute as well when the charged π is misidentified as an electron and when the decay is accompanied by a photon, either radiated from the electron or due to other accidental beam activity.

E799 utilized the existing beam line and detector of Fermilab experiment E731 with a few modifications. A description of the detector has been published previously [8]; however, the detector elements important to this analysis are discussed below. The two K_L beams were produced from an 800 GeV proton beam incident upon a beryllium target and traveled approximately 120 m in vacuum to the beginning of the decay volume. The average momentum of decaying K_L's in the decay volume was 50 GeV/c. The primary component of the detector for this analysis was the charged particle spectrometer consisting of a pair of drift chambers before and after an analyzing magnet which gave a momentum kick of 200 MeV/c transverse to the beam direction. Downstream of the spectrometer, an electromagnetic calorimeter 18.7 radiation lengths deep provided the photon detection capability. The calorimeter was composed of 804 lead glass blocks, each 5.8 cm by 5.8 cm in cross section, and had two 11.6 cm by 11.6 cm holes to allow passage of the K_L beams. A lead and lucite sampling calorimeter was placed 3 m behind the holes in the lead glass array for purposes of vetoing electrons and photons escaping down the beam holes of the lead glass calorimeter. A scintillator hodoscope with one vertically segmented plane followed by one horizontally segmented plane was placed between the charged spectrometer and calorimeter for the purpose of fast triggering capability. An additional scintillator bank was located behind the lead glass calorimeter to identify instances of energy leakage out of the back of the array associated with hadron activity. A lead wall was placed between the calorimeter and this hadron veto to terminate electromagnetic showers in the calorimeter and enhance the signal of hadron showers. Photon veto modules were located at a number of positions throughout the detector and decay volume.

The trigger for this search required (1) a coincidence of hits in the trigger hodoscope consistent with two tracks, (2) an analog sum of the lead glass calorimeter signals above a threshold of 6 GeV, (3) a veto of charged particle hits in any of the photon detector modules, (4) a number of "hit pairs" in each drift chamber consistent with two tracks, and (5) three distinguishable clusters of energy deposition, each greater than 2 GeV, in the calorimeter. Because of the high rate of events passing these requirements, the trigger was prescaled by a factor of 14. The rate was dominated by K_{e3} decays with radiative or accidental photons.

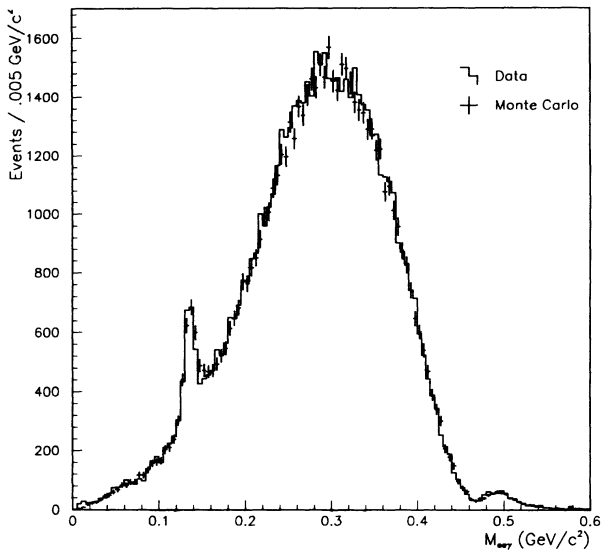

FIG. 1. Plot of $ee\gamma$ mass for data (histogram) and Monte Carlo simulation (crosses) before imposing kinematic cuts to eliminate the backgrounds. The majority of events come from K_{e3} decays with misidentified pions, producing the large hump at 300 MeV/c^2. The peak at 135 MeV/c^2 is due to $\Lambda \to n\pi^0$, $\pi^0 \to e^+e^-\gamma$ decays, while that at 500 MeV/c^2 is from K_L Dalitz decays.

In the off-line analysis, tracks were reconstructed from the drift chamber information and association of energy clusters in the calorimeter. Extra clusters which were not matched with tracks were assumed to have been deposited by photon candidates. Events with two tracks were then required to fit to a decay vertex. The fitted vertex was required to lie between 120 and 159 m downstream of the target, a region with good photon veto coverage. Background from $K_L \to \pi^0\pi^0\pi^0$, $\pi^0 \to e^+e^-\gamma$ and $K_L \to \pi^0\pi^0$, $\pi^0 \to e^+e^-\gamma$ was then rejected by discarding events with activity in the photon veto modules. The vertex uncertainty for signal π^0 Dalitz decays is typically large (1.4 m) due to the small opening angle between electron pairs, yet restricting the vertex location uncertainty to less than 3.0 m was necessary to limit the error in the P_t measurement, rejecting poorly reconstructed $\Lambda \to n\pi^0$, $\pi^0 \to e^+e^-\gamma$ decays.

Several cuts were imposed in order to reduce the number of K_{e3} background events. Electrons were identified by requiring that the cluster energy and track momentum

agree within 15% and that the transverse profile of each cluster energy distribution be consistent with that of a single electromagnetic shower. With the E799 detector 96% of electrons satisfied these requirements, compared to 2.5% of pions from K_{e3} decays. Because of the high rate of accidental activity in the lead glass blocks closest to the beam, only photons further than one block (5.8 cm) from the beam holes were analyzed. This further reduced the number of K_{e3} decays where an accidental photon accompanied the decay products. The distribution of the $ee\gamma$ invariant mass for the remaining data and sum of simulated decay modes is shown in Fig. 1. Dalitz decays of the neutral pion were selected by requiring that the ratio of the candidate electron-positron invariant mass to the total $ee\gamma$ invariant mass be less than 0.30. This cut rejects most of the K_{e3} events because the charged tracks in K_{e3} decays are not usually close to each other, as is the case in π^0 Dalitz decays. Furthermore, in π^0 Dalitz decays the photon is preferentially emitted back to back with the e^+e^- pair in the π^0 rest frame, whereas the photon in a radiative K_{e3} decay is emitted at a small angle with respect to the electron. Events were discarded if the sum of the cosines of the angle between the electron and photon and the angle between the positron and photon was greater than -1.5, where the angles have been computed in the $ee\gamma$ rest frame. The remaining K_{e3} background was rejected by requiring that the measured P_t be greater than the kinematic limit for $K^0 \to \pi^+ e^- \nu\gamma$, given by

$$P_t(\pi e\gamma) \leq \frac{m_{K^0}^2 - m_{\pi e\gamma}^2}{2m_{K^0}}.$$

Because of the pion assignment ambiguity in this analysis, there are two such limits. The measured P_t was required to be greater than both. This cut was also very effective at removing the $K_L \to \pi^+\pi^-\pi^0$, $\pi^0 \to \gamma\gamma$ background where only one photon was identified. The resulting plot of P_t and the $ee\gamma$ invariant mass, $m_{ee\gamma}$, is shown in Fig. 2 for the $K_L \to \pi^0\nu\overline{\nu}$ simulation and for the data. The final signal requirements were that $125 < m_{ee\gamma} < 145$ MeV/c^2 and $160 < P_t < 231$ MeV/c, consistent with a neutral pion of large P_t. No events from the data remained after this cut.

The level of background expected to contribute to the signal region was estimated by simulating each of the background sources. The $\Lambda \to n\pi^0$, $\pi^0 \to e^+e^-\gamma$ Monte Carlo events were normalized to the data in Fig. 1 in the range $120 < m_{e e\gamma} < 150$ MeV/c^2, $m_{ee}/m_{ee\gamma} < 0.3$, and $P_t < 120$ MeV/c. Background events from these Λ decays are clustered below the signal region in Fig. 2(b) and contribute fewer than 0.1 events to the signal box. The semileptonic K_{e3} Monte Carlo events were normalized to the $360 < m_{ee\gamma} < 460$ MeV/c^2 region of data in Fig. 1 where this mode is dominant. The K_{e3} background events appear in a diagonal band stretching from directly above down to the right side of the signal region in Fig. 2(b) and contribute less than 0.2 events. The

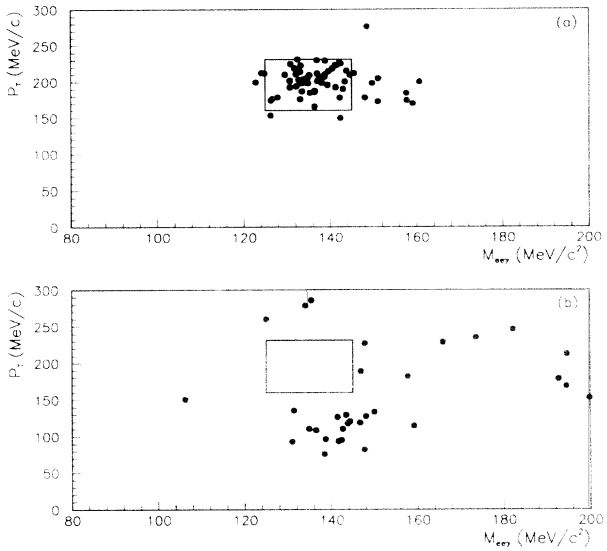

FIG. 2. Scatter plot of P_t versus $ee\gamma$ mass for (a) $K_L \to \pi^0\nu\overline{\nu}$ simulation and (b) data. No $K_L \to \pi^0\nu\overline{\nu}$ candidates were found in the data. Decays from $\Lambda \to n\pi^0$ are clustered below the signal box. The K_{e3} events populate the area to the right and above the signal region. A total of 0.6 ± 0.2 background events are expected in the signal box from the simulation. The plot of the $K_L \to \pi^0\nu\overline{\nu}$ simulation represents a hypothetical branching fraction equal to 20 times our upper limit.

$K_L \to \pi^+\pi^-\pi^0$ ($\pi^0 \to \gamma\gamma$ and $\pi^0 \to e^+e^-\gamma$) Monte Carlo events were normalized to the range $200 < m_{ee\gamma} < 360$ MeV/c^2 and $P_t < 80$ MeV/c of data in Fig. 1 after subtracting the contribution expected from K_{e3} decays. The $K_L \to \pi^+\pi^-\pi^0$ mode was easily rejected and contributed fewer than 0.1 events to the final plot. The $K_L \to \pi^0\pi^0$ and $K_L \to \pi^0\pi^0\pi^0$ Monte Carlo simulations were normalized using their known branching fractions and the integrated K_L decay flux determined by observing the decay $K_L \to e^+e^-\gamma$ as discussed below. The $K_L \to \pi^0\pi^0$, $\pi^0 \to e^+e^-\gamma$ background is kinematically similar to $K_L \to \pi^0\nu\overline{\nu}$ and is expected to contribute 0.5 ± 0.2 events to the signal region. The $K_L \to \pi^0\pi^0\pi^0$, $\pi^0 \to e^+e^-\gamma$ mode appears evenly distributed over the entire region of the final plot, because the detected photon is typically not from the $\pi^0 \to e^+e^-\gamma$ decay but from one of the other two π^0 decays. This background contributes 0.1 ± 0.1 events to the signal box. Altogether, 0.6 ± 0.2 background events are expected in the signal box of Fig. 2(b).

The Monte Carlo simulation was also used to determine the efficiency for detecting events from the signal mode $K_L \to \pi^0\nu\overline{\nu}$, $\pi^0 \to e^+e^-\gamma$. The generated spectrum for E_{π^0} in the K_L center of mass system was taken to be [1,9]

$$\frac{d\Gamma}{dE_{\pi^0}} \propto \left[1 + \frac{\lambda_+}{m_{\pi^0}^2}\left(m_K^2 + m_{\pi^0}^2 - 2m_K E_{\pi^0}\right)\right] \times \left(E_{\pi^0}^2 - m_{\pi^0}^2\right),$$

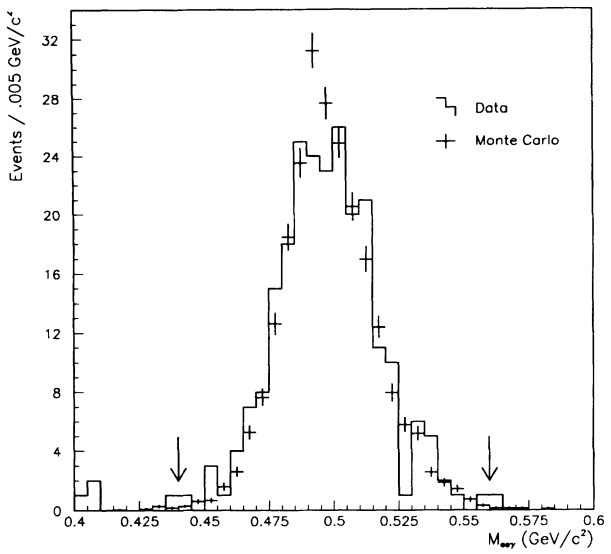

FIG. 3. Histogram of $ee\gamma$ mass for data and $K_L \to e^+e^-\gamma$ Monte Carlo. This mode is used to normalize the integrated K_L flux in the search for $K_L \to \pi^0\nu\bar{\nu}$, $\pi^0 \to e^+e^-\gamma$. There are 233 events in the selected mass region indicated by the arrows.

where the pion decay form factor $f_+(q^2)$ has been parametrized as $1 + \lambda_+ q^2/m_{\pi^0}^2$ with the measured value λ_+=0.032 [10]. This is the expected distribution calculated from the standard model.

The integrated K_L flux was determined by simultaneously reconstructing the K_L Dalitz mode, $K_L \to e^+e^-\gamma$, chosen because of its similarity to the signal mode in particle identification and geometric acceptance. That is, any uncertainty in electron identification efficiency and geometric acceptance canceled to first order in the ratio of detection efficiencies used for computing the branching fraction of the signal mode. The normalization mode was analyzed in parallel with the signal mode search with all the same requirements except $P_t < 60$ MeV/c (3σ) and $440 < m_{ee\gamma} < 560$ MeV/c^2 ($\pm 3\sigma$). Figure 3 shows the full data sample with 233 events in the selected mass region. Also shown are the results of the Monte Carlo simulation of $K_L \to e^+e^-\gamma$ normalized to the 233 events.

The single event sensitivity S for $K_L \to \pi^0\nu\bar{\nu}$ can be computed from the relation

$$S(K_L \to \pi^0\nu\bar{\nu}) = \frac{B(K_L \to e^+e^-\gamma)}{B(\pi^0 \to e^+e^-\gamma)} \frac{N_{\pi\nu\bar{\nu}}}{N_{ee\gamma}} \frac{\epsilon_{ee\gamma}}{\epsilon_{\pi\nu\bar{\nu}}},$$

where N_x is the number of observed events and ϵ_x is the net efficiency for accepting and identifying events of type x. The net efficiency for the $K_L \to e^+e^-\gamma$ mode was 0.83% while that for $K_L \to \pi^0\nu\bar{\nu}$, $\pi^0 \to e^+e^-\gamma$ was 0.11%. This difference in net efficiencies is due primarily to the greater deflection of electrons away from the calorimeter in $K_L \to \pi^0\nu\bar{\nu}$ ($\pi^0 \to e^+e^-\gamma$) decays than the typically more energetic electrons in $K_L \to e^+e^-\gamma$ decays by the analyzing magnet. The systematic uncertainty in determining the ratio of these net efficiencies was estimated by studying the effect of varying parameters associated with the calorimeter calibration and spectrometer calibration; however, the dominant source of systematic uncertainty contributing to $B(K_L \to \pi^0\nu\bar{\nu})$ was found to be the uncertainty in $B(K_L \to e^+e^-\gamma)$ of 5% [10]. The single event sensitivity for this search was $(2.48 \pm 0.16 \pm 0.19) \times 10^{-5}$, where the first uncertainty is statistical and the second is systematic. This implies $B(K_L \to \pi^0\nu\bar{\nu}) < 5.8 \times 10^{-5}$ at the 90% confidence level. This upper limit includes a correction due to the uncertainty in the single event sensitivity [11].

Our upper limit on the branching ratio of $K_L \to \pi^0\nu\bar{\nu}$ represents an improvement in sensitivity of roughly a factor of 4 compared to the previous limit [6]. Future rare kaon decay experiments will achieve greater sensitivity in the search for this mode with improvements in K_L flux, data acquisition capability to handle the high trigger rates, and background rejection. Of particular importance are hermetic photon veto systems and better e/π separation.

We wish to thank Gene Beck, John Krider, Harold Sanders, Peter Shawhan, Margherita Vittone, the Fermilab computing division, and the Fermilab accelerator division. Support was provided for this experiment by NSF and DOE. In addition, one of us (Y.W.W.) would like to acknowledge support from an O.J.I. grant from DOE, and another of us (A.R.B.) acknowledges the support of the Robert R. McCormick Foundation while at the University of Chicago.

* Present address: Seoul National University, Seoul 151-42, Korea.

[1] L. Littenberg, Phys. Rev. **D** 39, 3322 (1989).
[2] C.O. Dib, I. Dunietz, and F. J. Gilman, Phys. Rev. D **39**, 2639 (1989).
[3] C. Allieggro *et al.* , Phys. Rev. Lett. **68**, 278 (1992). This paper predicts the indirect part of $B(K_L \to \pi^0 e^+e^-) < 1.6 \times 10^{-12}$ based on their measurement of $B(K^+ \to \pi^+e^+e^-)$ and the model of G. Ecker, A. Pich, and E. de Rafael [Nucl. Phys. **B29**, 692 (1987)], which employs an effective chiral Lagrangian.
[4] L. Wolfenstein, Phys. Rev. Lett. **51**, 1945 (1983).
[5] C.S. Kim, J.L. Rosner, and C.-P. Yuan, Phys. Rev. D **42**, 96 (1990).
[6] G. E. Graham *et al.*, Phys. Lett. B **295**, 169 (1992).
[7] D. A. Harris *et al.*, Phys. Rev. Lett. **71**, 3918 (1993).
[8] K. S. McFarland *et al.*, Phys. Rev. Lett. **71**, 31 (1993). The E799 detector is illustrated in Fig. 1 of this reference. A detailed description can also be found in M. Weaver, UCLA Ph.D. thesis, 1994 (unpublished).
[9] N. G. Deshpande and G. Eilam, Phys. Rev. Lett. **53**, 2289 (1984).
[10] K. Hikasa *et al.*, Particle Data Group, Phys. Rev. D **45**, S1 (1992).
[11] R. D. Cousins and V. L. Highland, Nucl. Instrum. Methods Phys. Res., Sect. A **320**, 331 (1992).